Increased Levels of Inosine in a Mouse Model of Inflammation

ARTICLE *in* CHEMICAL RESEARCH IN TOXICOLOGY · MARCH 2013

Impact Factor: 3.53 · DOI: 10.1021/tx300473n · Source: PubMed

9 AUTHORS, INCLUDING:

Aswin Mangerich

Universität Konstanz

37 PUBLICATIONS **321** CITATIONS

SEE PROFILE

Jose L Mcfaline

Massachusetts Institute of Technology

12 PUBLICATIONS **554** CITATIONS

SEE PROFILE

Koli Taghizadeh

Massachusetts Institute of Technology

68 PUBLICATIONS **2,298** CITATIONS

SEE PROFILE

Peter C Dedon

Massachusetts Institute of Technology

173 PUBLICATIONS **5,377** CITATIONS

SEE PROFILE

Published in final edited form as:
Chem Res Toxicol. 2013 April 15; 26(4): 538–546. doi:10.1021/tx300473n.

Increased levels of inosine in a mouse model of inflammation

Erin G Prestwich[†], **Aswin Mangerich**[†,‡], **Bo Pang**[†,⊥], **Jose L McFaline**[†,ς], **Pallavi Lonkar**[†,§], **Matthew R Sullivan**[†], **Laura J Trudel**[†], **Koli Taghizedeh**[¶], and **Peter C Dedon**[†,¶,*]

[†]Department of Biological Engineering, Massachusetts Institute of Technology, 77 Massachusetts Avenue, Cambridge, MA 02193

[¶]Center for Environmental Health Science, Massachusetts Institute of Technology, 77 Massachusetts Avenue, Cambridge, MA 02193

[‡]Department of Biology, University of Konstanz, D-78457 Konstanz, Germany

Abstract

One possible mechanism linking inflammation with cancer involves the generation of reactive oxygen, nitrogen and halogen species by activated macrophages and neutrophils infiltrating sites of infection or tissue damage, with these chemical mediators causing damage that ultimately leads to cell death and mutation. To determine the most biologically deleterious chemistries of inflammation, we previously assessed products across the spectrum of DNA damage arising in inflamed tissues in the SJL mouse model nitric oxide over-production (Pang *et al.*, *Carcinogenesis* 28: 1807–1813, 2007). Among the anticipated DNA damage chemistries, we observed significant changes only in lipid peroxidation-derived etheno adducts. We have now developed an isotope-dilution, liquid chromatography-coupled, tandem quadrupole mass spectrometric method to quantify representative species across the spectrum of RNA damage products predicted to arise at sites of inflammation, including nucleobase deamination (xanthosine, inosine), oxidation (8-oxoguanosine), and alkylation (1,N^6-etheno-adenosine). Application of the method to liver, spleen, and kidney from the SJL mouse model revealed generally higher levels of oxidative background RNA damage than was observed in DNA in control mice. However, compared to control mice, RcsX treatment to induce nitric oxide overproduction resulted in significant increases only in inosine and only in the spleen. Further, the nitric oxide synthase inhibitor, N-methylarginine, did not significantly affect the levels of inosine in control and RcsX-treated mice. The differences between DNA and RNA damage in the same animal model of inflammation point to possible influences from DNA repair, RcsX-induced alterations in adenosine deaminase activity, and differential accessibility of DNA and RNA to reactive oxygen and nitrogen species as determinants of nucleic acid damage during inflammation.

Keywords

inflammation; nitric oxide; macrophage; mass spectrometery; RNA

[*]Address all correspondence to: Peter C. Dedon, Dept. of Biological Engineering, 56-787B, 77 Massachusetts Avenue, Cambridge, MA 02139; tel: +1-617-253-8017; pcdedon@mit.edu.
[⊥]Present address: Alnylam Pharmaceuticals, 300 Third Street, 3rd Floor, Cambridge, MA 02142
[ς]Present address: Dept. of Biology, Massachusetts Institute of Technology, Cambridge, MA 02139
[§]Present address: Catabasis Pharmaceuticals, Inc., One Kendall Square, Bldg. 1400E, Suite B14202, Cambridge, MA 02139

INTRODUCTION

Chronic inflammation is now recognized as a cause of human disease.[2–4] Current evidence points to a persistent local inflammatory state in organ-specific carcinogenesis,[5–7] with >16% of all cancers caused by chronic infection or other types of chronic inflammation.[8] This is illustrated by the causal relationship of *Heliobactor pylori* infection and gastric cancer,[9, 10] viral hepatitis and liver cancer,[11] and *Schistosoma haematobium* infection and bladder cancer.[12, 13] Despite this evidence, the mechanisms underlying the link between chronic inflammation and cancer have not been clearly defined. In addition to cytokine-mediated changes in host cell cycle and apoptosis, the infiltration of macrophages and neutrophils at sites of inflammation leads to the generation of a variety of reactive oxygen and nitrogen species that cause damage to all types of biological molecules.[14, 15] Activated macrophages produce nitric oxide (NO)[15, 16] that acts is a signaling molecule and regulator of the cardiovascular, nervous, and immune systems at nanomolar concentrations.[17, 18] At higher concentrations approaching 1 μM,[15, 17] NO is considered pathological due to interference with signaling pathways and by reactions with oxygen and superoxide ($O_2^{\bullet-}$) to generate a variety of reactive nitrogen species.[15, 19] Autooxidation of NO generates the nitrosating agent, nitrous anhydride (N_2O_3), while the reaction of $O_2^{\bullet-}$ and NO at diffusion-controlled rates leads to peroxynitrite ($ONOO^-$), which, in its protonated form, undergoes rapid ($t_{1/2}$ ~1 s) homolysis to yield hydroxyl radical ($^{\bullet}OH$) and the weak oxidant, nitrogen dioxide radical ($NO_2^{\bullet}$). Further reaction of $ONOO^-$ with carbon dioxide forms nitrosoperoxycarbonate ($ONOOCO_2^-$) that also undergoes homolytic scission to form carbonate radical anion ($CO_3^{\bullet-}$) and $NO_2^{\bullet}$.

With implications for carcinogenesis and the development of biomarkers of inflammation, these reactive oxygen and nitrogen species readily react with nucleic acids, proteins, lipids, and carbohydrates to form nucleic acid damage products covering a range of chemistries; nucleobase damage products studied here are shown in Figure 1. Our previous work demonstrated that nitrosation of DNA nucleobases by N_2O_3 leads to the conversion of guanine to either xanthine (X; Fig. 1) or oxanine (O), and adenine to hypoxanthine (I; Fig. 1).[15] DNA is also subject to oxidation and nitration by reactive nitrogen species, mainly as a consequence of reactions with $ONOO^-$ and $ONOOCO_2^-$. While $ONOO^-$ causes mainly 2-deoxyribose oxidation in DNA,[20] the presence of millimolar concentrations of carbon dioxide in tissues leads to the formation of $ONOOCO_2^-$ that gives rise to $CO_3^{\bullet-}$ that preferentially oxidizes guanine in DNA.[15] The resulting oxidation products include primary lesions such as 8-oxo-7,8-dihydroguanine (8-oxo-G; Fig. 1), as well as a variety of secondary products of 8-oxo-G oxidation.[15] These DNA lesions that arise from direct reaction of oxidants with DNA stand in contrast to adducts arising indirectly from reactions of DNA bases with electrophiles derived from primary oxidations of polyunsaturated fatty acids and other cellular molecules.[21] For example, lipid peroxidation induces the formation of a variety of α,β-unsaturated aldehydes such as *trans*-4-hydroxy-2-nonenal, acrolein, 4,5-epoxy-2(E)-decenal, and 4-hydroperoxy-2(E)-nonenal.[21, 22] These electrophiles can react with nucleobases to form many alkylated products including substituted and unsubstituted etheno adducts, such as 1,N^6-ethenoadenine (εA) shown in figure 1.[21, 22]

We recently reported analyses of nucleic acid damage products in two different mouse models of inflammation. [1, 23] In the $Rag2^{-/-}$ infection-induced colitis model, infected animals exhibited higher levels of chlorinated nucleic acid lesions, and increased hypoxanthine levels in DNA.[23] The current work was inspired by the analysis of DNA lesions in the SJL mouse model of inflammation, which was conducted to define the predominant chemical damage pathway.[1] In this model, injection of superantigen-bearing, reticulum cell sarcoma-derived RcsX cells leads to widespread activation of macrophages with subsequent generation of large quantities of NO, $O_2^{\bullet-}$, and secondary reactive species

in spleen, lymph nodes, and liver, with a maximal 30- to 40-fold increase in urinary nitrate excretion at 12–14 days.[24–27] The generation of reactive species is associated with an increased mutation frequency[24] and protein damage in the form of nitrotyrosine[24] and lipid peroxide adducts.[28] Among the variety of potential DNA damage products, we observed significant increases in only the etheno adducts (Figure 1).[1, 29] The limited changes in other damaged nucleobases could result from (1) interception of reactive oxygen and nitrogen species prior to their entry into the nucleus, for example by reaction with glutathione; (2) efficient DNA repair processes that obviate changes in the steady state levels of the lesions; and (3) protection of duplex DNA from reactions by virtue of the less solvent exposed nature of the nucleobases compared to single-stranded nucleic acids or nucleosides. Because RNA differs from DNA in these aspects, we undertook an analysis of similar damage products in RNA isolated from SJL mouse tissues to test these hypotheses.

RNA represents a significantly different target for damage by the chemical mediators of inflammation. Though RNA is hydrolytically more labile, it is chemically more stable than DNA.[30] However, there are other characteristics that make it more prone to chemical reactions intracellularly. RNA is largely single stranded, leading to greater solvent acessibility of most nucleobases in RNA. RNA is also more widely distributed in cells, located both in the nucleus and cytoplasm where it can be exposed to exogenous toxicants and possible endogenous reactive oxygen species from mitochondria.[31] There is also a paucity of repair processes for most RNA damage products, with oxidative dealkylation via AlkB being the only confirmed repair pathway.[32, 33] Turnover rates differ widely between DNA and RNA, with DNA being relatively stable in non-dividing cells, whereas RNA turnover rates vary between a matter of minutes or hours for mRNA to rRNA that persists for several days.[34] There are also generally larger quantities of RNA relative to DNA in most cell types.[35] These differences motivated us to measure RNA damage in the SJL mouse model of NO over-production and inflammation.

MATERIALS AND METHODS

Materials

All chemicals and reagents used were of the highest purity available and were used without further purification unless otherwise noted. Phosphodiesterase I was purchased from US Biologicals (Cleveland, OH). Tetrahydrouridine and N^G-methyl-L-arginine were purchased from Calbiochem (San Diego, CA). Benzonase, calf intestine alkaline phosphatase, butylated hydroxytoluene, deferoxamine mesylate, and other buffer salts were purchased from Sigma Chemical Company (St Louis, MO). Coformycin was obtained from the National Cancer Institute Chemical Carcinogen Reference Standards Repository. Omnisolv HPLC-grade acetonitrile was purchased from EMD (Gibbstown, NJ) for LC-MS/MS analyses. Water purified through a Milli-Q system (Millipore Corp., Bedford, MA) was used throughout our studies. RNeasy Midi kits and RNAlater RNA stabilization reagent were purchased from Qiagen (Hilden, Germany). Centrifugal membrane filters were purchased from Pall Corporation (Northborough, MA). Isotopically labeled [$^{15}N_5$]-rG and [$^{15}N_5$]-rA were purchased from Spectra Stable Isotopes or Cambridge Isotopes (Andover, MA).

Synthesis of isotopically-labeled internal standards

Syntheses of [$^{15}N_4$]-labeled xanthosine (rX), inosine (rI), [$^{15}N_5$]-1,N^6-etheno-adenosine (εrA), and [$^{15}N_5$]-8-oxo-7,8-dihydroguanosone (8-oxo-rG) were performed as described elsewhere.[36–41] All standards were purified by reversed-phase HPLC, with retention times agreeing with unlabeled standards, characterized by HPLC-coupled electrospray ionization time-of-flight mass spectrometry, and quantitated by UV absorbance using published exctinction coefficients.[36–41]

Experiments with SJL mice

All studies using mice were performed in accordance with protocols approved by the MIT Committee on Animal Care and with the NIH *Guide for the Care and Use of Laboratory Animals*. RcsX cells (kindly supplied by Dr. N. Ponzio, University of New Jersey Medical Center, Newark, NJ) were passaged through SJL mice (Jackson Laboratory, Bar Harbor, ME) and harvested from lymph nodes 14 days after inoculation, according to published procedures.[24] Cells were manually dissociated from lymph nodes followed by washing in phosphate-buffered saline (PBS; 140 mM NaCl, 2.7 mM KCl, 10 mM Na_2HPO_4, 1.8 mM KH_2PO_4, pH 7.4) and freezing in aliquots of 5×10^7 cells in 10% dimethylsulfoxide/fetal bovine serum. To stimulate NO production, groups of 12 SJL mice (5–6 w old) were injected intra-peritoneally with 10^7 RcsX cells in 200 μL of PBS, and control mice were injected with 200 μL PBS. Parallel studies were performed in control and RcsX-treated mice that were also treated with the inducible nitric oxide synthase (iNOS) inhibitor, N^G-monomethyl-L-arginine (NMA), which was administered in drinking water (30 mM) *ad libitum* during the duration of the study. On day 12 after injection of RcsX cells, treated and control were euthanized (carbon dioxide) and the spleen, liver and kidneys were removed, divided into 30–50 mg pieces, submerged in RNA stabilization reagent (RNAlater), and snap frozen in liquid nitrogen and stored at −80 °C. Analysis of RNA damage products was performed on 6–9 mice in each group, with the remaining tissues used in other studies.

RNA isolation

RNA was isolated from spleen, liver, and kidney tissue using the RNeasy Midi kit following the manufacturer's instructions with additional steps added in order to reduce adventitious damage during the isolation. Briefly, 100 mg samples of frozen tissue were placed in 2 mL of RLT lysis buffer containing 3.5 μM coformycin (adenine deaminase inhibitor), 2.5 mM deferoxamine mesylate (metal-chelating antioxidant), 0.5 mM butylated hydroxytoluene (antioxidant), and 0.2 mM tetrahydrouridine (cytosine deaminase inhibitor), and homogenized for 1–2 min using a Qiagen Tissue Ruptor on a medium setting. RNA concentration was determined by UV spectroscopy and samples were stored at −80 °C prior to analysis. The quantity of RNA analyzed was corrected for concentration and contaminating DNA by measuring canonical ribonucleosides during the HPLC pre-purification step described shortly and comparing the areas under the curve for each nucleoside with calibration curves obtained with standards.

Quantification of RNA damage products

Nucleoside forms of RNA damage products were quantified using a liquid chromatography-coupled tandem mass spectrometry (LC-MS/MS) method derived from that developed for DNA by Pang *et al.*[1] RNA (50–100 μg) was digested to nucleoside form by overnight reaction (37 °C) in 200 μL of 10 mM Tris (pH 7.8) with 1 mM $MgCl_2$, 4 U of Benzonase, 17 U of alkaline phosphatase, 0.2 U of phosphodiesterase I, 3.5 μM coformycin, 2.5 mM deferoxamine mesylate, 0.5 mM butylated hydroxytoluene and 0.2 mM tetrahydrouridine, and a mixture of internal standards: 10 pmol $^{15}N_5$-rX and $^{15}N_4$-rI; and 1 pmol of $^{15}N_5$-8-oxo-rG and ^{15}N-εrA. Enzymes were subsequently removed by microfiltration (10kD, Nanosep Omega) and the filtrate was concentrated under vacuum. Ribonucleosides were resolved by HPLC on an Agilent 1100 HPLC equipped with a Varian microsorb C18 reversed-phase column (250 × 4.6 mm, 5 μm particle size, 100 Å pore size; Palo Alto, CA), a thermostatted column compartment, an diode array detector and a fraction collector. Elution was performed at 9 °C with a gradient of acetonitrile in 8 mM ammonium acetate buffer following the details in Table S1. Individual ribonucleosides were fractionated by HPLC bracketing empirically determined elution times for each damage product shown in Table S2. The ribonucleoside-containing fractions were dried under vacuum, redissolved in

50 μL of water and analyzed by LC-MS/MS. The fractions containing rX, 8-oxo-rG, and the etheno adducts were injected separately onto a reversed-phase HPLC column (Thermo hypersil gold AQ C18 column; 150 × 2.1 mm, 3 μm particles) eluted isocratically at a flow rate of 200 μL/min with a mobile phase consisting of 0.1% acetic acid with low percentages of acetonitrile, as detailed in Table S2. The fraction containing rI was injected on a YMC-Pack ODS-AQ column (3 μm particles, 12 nm pores) and eluted with a mobile phase of 0.1% acetic acid with a gradient of 0.5–70% acetonitrile over 30 min. In all cases, the HPLC eluent was directed into an AB Sciex API 3000 triple quadrupole mass spectrometer operated in positive ion mode, with the instrument parameters shown in Table S2. Multiple reaction monitoring (MRM) was performed with the first quadrupole (Q1) set to transmit the precursor ions and third quadrupole (Q3) set to monitor the deglycosylated fragment ions shown in Table S2. Quantification of ribonucleosides was accomplished using linear calibration curves ($r^2 > 0.95$, data not shown). To determine LOQ values with appropriate matrix effects, 100 μg of SJL kidney RNA was hydrolyzed without the addition of internal standards and HPLC fractions were collected at the retention times for the desired damaged nucleosides, with internal standards then spiked into the appropriate HPLC fractions for subsequent quantification by LC-MS/MS. To determine whether artifactual deamination occurred, 25 μg of rA was subjected to digestion conditions, HPLC pre-purification, and LC-MS/MS analysis as noted above in the presence or absence of the adenosine deaminase inhibitor, coformycin. The results shown in Table S4 confirm the absence of deamination artifacts, as observed in previous studies.[1]

RESULTS AND DISCUSSION

The present studies were motivated by the observation of limited increases in DNA damage induced by inflammation in the SJL mouse model of NO overproduction.[1] While εdA and 1,N^2-εdG were elevated 3- to 4-fold in spleen, liver, and kidney in the RcsX-treated mice, there were no significant changes in the levels of products arising from nitrosative deamination or direct oxidation.[1] To determine whether the different cellular conditions of RNA would lead to higher levels of inflammation-induced damage and a different spectrum of damage chemistries, we developed an LC-MS/MS method to quantify RNA lesions representative of the deamination, oxidation, and alkylation chemistries of inflammation and applied it to tissues from the SJL mouse model.

Development of a method to quantify RNA damage products

The key feature of these studies was the development of a sensitive, accurate, and precise analytical method to quantify RNA damage products representing several chemistries predicted to occur with the reactive nitrogen species of inflammation. The critical first step in the method involves RNA isolation and manipulation, with careful attention to minimize adventitious damage caused by deaminase enzymes contaminating commercial enzyme preparations[36, 42] and by oxidation of rG and 8-oxo-rG.[15, 43] These artifacts were minimized by the addition of nucleobase deaminase inhibitors (coformycin, tetrahydrouridine), a metal chelator (deferoxamine), and an antioxidant (BHT), to buffers used during RNA isolation and processing.

Another critical facet of the method involved the chromatographic resolution of the ribonucleosides. As shown in Figure 2 for the first dimension pre-purification chromatographic step, damaged ribonucleosides were well resolved from each other and from canonical ribonucleosides. Any co-eluting canonical and damaged ribonucleosides in fractions collected from the first HPLC column were subsequently completely resolved on a second HPLC system for LC-MS/MS analysis. This level of chromatographic resolution was critical for the deaminated nucleobase products rI and rX, which are only one mass unit

larger than their canonical counterparts, and for 8-oxo-rG that has the potential to arise from oxidation of rG in the electrospray source.

To ensure the highest sensitivity for each damage product, the parameters for MS/MS MRM analysis were optimized using standards for each analyte (Table S2). The recovery of internal standards relative to unprocessed samples was calculated to demonstrate the importance of the addition of internal standard to account for loss and matrix effects (Table S3). While the overall recovery of ribonucleosides was variable (Table S3), the limits of detection (fmol) range from 1–50 fmol (Table S2), which amounts to 0.2–25 lesions per 10^8 nt in 50 μg of RNA.

Quantification of RNA lesions in SJL mouse tissues: predominance of rI

In the SJL mouse model of NO overproduction and systemic inflammation, injection of RcsX tumor cells leads to macrophage activation, with associated increases in NO and $O_2^{\bullet -}$ and maximal phagocyte infiltration occurring in the spleen and to a lesser extent the liver at 12–14 days post-injection.[25] Using the LC-MS/MS method, we quantified a set of ribonucleoside damage products thought to reflect the spectrum of chemistries arising at sites of inflammation. The results of the analyses are shown in Table 1. The first observation was that only rI in the spleen was significantly elevated in the RcsX-treated mice (Figure 3). Further, administration of the iNOS inhibitor, NMA, to inhibit NO production[24] did not affect RNA damage levels in either control or RcsX-treated SJL mice. It is unlikely that the elevated rI levels resulted from adventitious deamination during RNA processing, as observed in previous studies with DNA,[36] since we included an adenosine deaminase inhibitor (coformycin) during RNA processing, with control experiments demonstrating the lack of adventitious deamination under the conditions of our experiments (Table S4).

As illustrated in Figure 4, there are several possible mechanisms that could cause levels of rI to increase in the spleen of SJL mice: nitrosative or enzymatic deamination of rA, nitrosative damage to the nucleotide pool or altered nucleotide metabolism, and RcsX cell-induced shifts in the population of cells comprising the SJL spleen. The first mechanism involves the aniticipated nitrosative deamination of nucleic acids by NO-derived N_2O_3.[15] While N_2O_3 causes deamination of DNA in cells exposed to physiologically relevant concentrations of NO,[44] there was no change in the steady-state level of dI, dX, dU, or dO in spleen, liver and kidney from RcsX-treated SJL mice.[1] Nitrosative deamination as the primary cause of rI formation is unlikely given the lack of increase in rX and the absence of an affect of NMA-induced inhibition of iNOS (Table 1).

Enzymatically-mediated RNA deamination is another potential source of endogenous rI formation. Among the possible enzymes are adenosine deaminases acting on double-stranded RNA (ADARs), which act on rA in unspliced transcripts,[45–47] and a family of ADAR-related adenosine deaminases that act on tRNA (ADAT or Tad).[48, 49] We recently observed that chemical stresses lead to altered levels of the two-dozen enzymatically modified ribonucleosides in tRNA, with modest (7–18%) increases in rI in tRNA caused by exposure of cells to the neutrophil-derived oxidizing and halogenating agent, HOCl.[50] It is likely that enzymatically-mediated alterations of rI in tRNA do not fully account for the observed increase of rI in total RNA, since tRNA accounts for ~10–15% of total cellular RNA, and even less in our samples given that our RNA isolation method favors species >300 nts.[51] Cytidine deaminase is also induced in response to cytokines and has been correlated to chronic inflammation and carcinogenesis,[42,45,46] though increased dU levels were not observed in previous studies of the SJL mouse model.[1] We did not quantify cytidine deamination in this study given the abundance of uridine as a canonical ribonucleotide.

This raises the possibility that ADARs may contribute to increased rI in the SJL mouse spleen. ADAR activity varies as a function of tissue type[52, 53] and rI is present in mRNA in tissue-specific levels that correlate with ADAR expression,[54] which may explain the observation of increased rI in spleen but not liver or kidney. With regard to inflammation, ADAR1 was previously found to be upregulated in stimulated macrophages,[55] and rI was found to increase in mRNA from splenic tissue from endotoxin-treated mice.[56, 57] Further, A-to-I editing in mRNA has also been found to increase in other stress conditions such as hypoxia.[58] Given the massive infiltration of activated macrophages observed in the spleen of RcsX-treated SJL mice, it is possible that elevated ADAR activity in stimulated macrophages accounts for the increased rI in spleen (Table 1).

Another possible mechanism for the inflammation-induced increase in rI in RNA involves the nucleotide pool. Purine nucleotide metabolism involves enzymatically-mediated conversion of nucleotides containing I and X, to A and G, respectively. We recently observed that defects in purine nucleotide metabolism lead to large increases in incorporation of I, but not X, into DNA and RNA, presumably as a result of increased levels of dITP/rITP and dXTP/rXTP in the nucleotide pool with selective incorporation of I-containing nucleotides into DNA and RNA by polymerase activity.[59] So the increase in rI could be caused by increased levels of rITP in the nucleotide pool, either as a result of altered purine nucleotide metabolism or nitrosative deamination of rATP. Since dI amounts remained constant in the SJL mice,[1] inflammation-induced alteration of purine nucleotide metabolism is unlikely. However, pertubations of nucleotide metabolism appear to affect levels of rI more than dI,[59] so smaller metabolic changes could be observed only in RNA. Nonetheless, the lack of an NMA effect suggests that nitrosative stress is not causing deamination of purines in the nucleotide pool.

The differences in RNA deamination levels could also be due to differences in RNA content of infiltrating immune cells (Fig. 4D,E), with RcsX treatment of the SJL mice leading to increased splenic mass due to infiltration of macrophages and other immune cells.[25] For example, higher levels of circulating nucleic acids, including DNA, mRNA, and miRNA, have been detected in humans and mouse models of cancer and inflammatory conditions.[63–67] High molecular weight DNA and RNA have also been found to be released from eukaryotic cells in tissue culture.[68] These extracellular nucleic acids can be phagocytized,[69] with inosine detected in internalized circulating RNAs possibly as a result of adenosine deamination during circulation or following phagocytosis (Fig. 4D).[70] Thus, higher levels of circulating nucleic acids in macrophages in the RcsX-treated animals could affect the observed levels of rI in the spleen. Another possible mechanism involves differences in RNA content in the spleen as a result of the large shift in cell composition following RcsX treatment (Fig. 4E). RNA synthesis generally increases along with cell volume, resulting in higher ratios of RNA to DNA in liver versus spleen,[35] with the RNA/DNA ratio lower in human lymphocytes than other cells (0.3 versus 4–6) and lower yet in leukemic lymphocytes.[60,61,62] These differences in cellular RNA content between the infiltrating and normal cell constiuents could also dilute potential differences in the other RNA damaged species in spleen and liver.

In any event, the specific mechanism underlying the increase in rI awaits clarification (Fig. 4). That RNA damage has consequences for cell viability is now widely recognized, beyond the obvious fact that RNA damage can disrupt protein synthesis and cause errors in protein translation.[71, 72] The damaged RNA may also have effects beyond the transcript itself in that proteins termed vigilins bind to promiscuously A-to-I-edited transcripts and target them, or their degradation products, to heterochromatic regions of the nucleus.[73] Further, altered levels of tRNA modifications can cause significant effects on protein translation.[74]

Understanding the mechanisms of RNA editing is essential in the study of inflammation, as inflammatory cytokines and iNOS are regulated post-transcriptionally at the level of nuclear export, localization and decay of mRNA. The 3'-untranslated regions (3'-UTR) of mRNA, which are key to the degradation process by facilitating the binding of regulatory proteins,[75, 76] contain AU-rich elements that are also the targets for ADARs that convert A-to-I. Thus, deamination could alter the inflammatory process by affecting the the binding of mRNA stabilizing and destabilizing proteins to cytokine and iNOS transcripts.[75, 77] For example, the fact that rI is commonly misread as rG[78] could affect the binding of AU-recognizing proteins that mark iNOS for exosomal degradation by binding to the 3'-UTR of mRNA.[79–81] Indeed, the binding of one such protein, KSRP, to iNOS mRNA can be disrupted if the AU binding region is replaced with GC.[79] Consequently, A-to-I editing could interfere with the degradation of cytokine and iNOS transcripts, perpetuating the inflammatory process. This is suggested by the abnormally high levels of ADAR1 in some pediatric leukemias,[82] with conditional deletion of ADAR1 causing regression of established myelogenous leukemia.[83] Thus, it appears that ADAR1 and A-to-I editing could perpetuate chronic inflammation and cancer.

Higher levels of RNA oxidation than DNA oxidation

In agreement with previous observations in other systems,[31] levels of oxidative damage to RNA are higher than in DNA in the SJL mouse model (Table 2).[1] Higher steady-state levels of 8oxorG than 8oxodG in cells and tissues have been observed by several groups,[23, 31, 84–86] while exposure to endogenous and exogenous electrophiles futher demonstrates the susceptibility of RNA to damage in cells and tissues. For example, benzo[a]pyrene, aflatoxin B1, and nitrosopyrrolidine adduct formation *in vivo* occurs at higher levels in RNA than DNA,[87–90] and etheno adduct formation is higher in RNA in ethyl carbamate-treated mice.[91] Oxidative stress also appears to affect RNA more than DNA,[31] as suggested by 8-oxoG levels in cells treated with H_2O_2[84] and in tissues from mice treated with 2-nitropropane,[92] 35-fold higher levels of lipid peroxidation-derived nucleobase adducts in exposed cells,[93] and higher levels of nucleobase chlorination products in cells exposed to HOCl.[94] Additionally, ~10-fold increases in 8-oxorG over 8-oxodG were observed in plasma and urine samples in a mouse model of aging, with modest increases in RNA oxidation observed in different tissue types.[95] The most likely explanations for the higher steady-state levels of RNA damage is a combination of greater accessibility to toxicants as a result of broader cellular distribution, greater solvent exposure of nucleobases in RNA due to the higher proportion of single-stranded structures, and more limited repair of the various RNA lesions. For DNA, nuclear concentrations of the various chemical mediators of inflammation may not be high enough to achieve significant reactivity with the histone-protected nucleobases, and those lesions that do form may be efficiently removed by robust DNA repair mechanisms. Apart from oxidative dealkylation by AlkB homologs,[32, 33] repair of deamination, oxidation, and chlorination products in RNA has not been described. Furthermore, differences in preventative repair in the form of nucleotide hydrolases such as *E. coli* MutT[96] and RdgB[97] and mammalian ITPA[98] that remove ribo- and 2-deoxyribonucleotide tri-and diphosphates from the nucleotide pool could conceivably account for the different levels of damage in DNA and RNA, but the enzymes appear to be reactive with both forms of nucleotide triphosphates.[96–98]

In summary, we have developed an isotope-dilution LC-MS/MS method to quantify RNA damage products across the spectrum of chemistries thought to arise at sites of inflammation, with application of the method to tissues from the SJL mouse model of NO over-production and inflammation. The results revealed that steady-state levels of RNA oxidation occurred at higher levels than were observed with DNA lesions from the same

mouse model, and that inflammation caused significant increases only in rI in spleen, possibly due to enzymatic deamination.

Supplementary Material

Refer to Web version on PubMed Central for supplementary material.

Acknowledgments

FUNDING SUPPORT

This work was supported by grants from the National Cancer Institute (CA116318, CA026731). Mass spectrometry studies were performed in the Bioanalytical Facilties Core of the MIT Center for Environmental Health Sciences, which is supported by a Center Grant from the National Institute of Environmental Health Sciences (ES002109). EGP was supported by 5T32-ES007020-34 NIEHS Training Grant in Environmental Toxicology. AM was supported by a fellowship of the German Academic Exchange Service (DAAD).

ABBREVIATIONS

SJL	Swiss Jim Lambert mouse
RcsX	superantigen bearing pre-B cell lymphoma cells
NO	Nitric oxide
$O_2^{\bullet-}$	superoxide
N_2O_3	nitrous anhydride
$ONOO^-$	peroxynitrite
$^{\bullet}OH$	hydroxyl radical
$NO_2^{\bullet}$	nitrogen dioxide radical
$ONOOCO_2^-$	nitrosoperoxycarbonate
$CO_3^{\bullet-}$	carbonate radical anion
X	xanthine
rX	xanthosine
dX	2’deoxyxanthosine
O	oxanine
dO	2’deoxyoxanine
I	hypxanthine
rI	inosine
dI	2’deoxyinosine
8-oxo-G	8-oxo-7,8-dihydroguanine
8-oxo-rG	8-oxo-7,8-dihydroguanosine
8-oxo-dG	8-oxo-7,8-dihydro-2’deoxyguanosine
εA	$1,N^6$-ethenoadenine
εrA	$1,N^6$-ethenoadenosine
NMA	N^G-monomethyl-L-arginine

rG	guanosine
rA	adenosine
iNOS	inducible nitric oxide synthase
LC–MS/MS	liquid chromatography-coupled tandem mass spectrometry
rATP	adenosine triphosphate
rITP	inosine triphosphate
dITP	2’deoxyinosine triphosphate
dXTP	2’deoxyxanthosine triphosphate
XTP	xanthosine triphosphate

REFERENCES

1. Pang B, Zhou X, Yu H, Dong M, Taghizadeh K, Wishnok JS, Tannenbaum SR, Dedon PC. Lipid peroxidation dominates the chemistry of DNA adduct formation in a mouse model of inflammation. Carcinogenesis. 2007; 28:1807–1813. [PubMed: 17347141]
2. Hussain SP, Harris CC. Inflammation and cancer: an ancient link with novel potentials. Int. J. Cancer. 2007; 121:2373–2380. [PubMed: 17893866]
3. Schottenfeld D, Beebe-Dimmer J. Chronic inflammation: a common and important factor in the pathogenesis of neoplasia. Cancer J. Clinic. 2006; 56:69–83.
4. Reuter S, Gupta SC, Chaturvedi MM, Aggarwal BB. Oxidative stress, inflammation, and cancer: How are they linked? Free Radic. Biol. Med. 2010; 49:1603–1616. [PubMed: 20840865]
5. Itzkowitz SH, Yio X. Inflammation and cancer IV. Colorectal cancer in inflammatory bowel disease: the role of inflammation. Am. J. Physiol. Gastrointest. Liver Physiol. 2004; 287:G7–G17. [PubMed: 15194558]
6. Nelson WG, De Marzo AM, DeWeese TL, Isaacs WB. The role of inflammation in the pathogenesis of prostate cancer. J Urol. 2004; 172:S6–S11. [PubMed: 15535435]
7. Whitcomb DC. Inflammation and Cancer V. Chronic pancreatitis and pancreatic cancer. Am. J. Physiol. Gastrointest. Liver Physiol. 2004; 287:G315–G319. [PubMed: 15246966]
8. de Martel C, Ferlay J, Franceschi S, Vignat J, Bray F, Forman D, Plummer M. Global burden of cancers attributable to infections in 2008: A review and synthetic analysis. Lancet Oncol. 2012; 13:607–615. [PubMed: 22575588]
9. Ebert MP, Yu J, Sung JJ, Malfertheiner P. Molecular alterations in gastric cancer: the role of Helicobacter pylori. Eur. J. Gastroenterol. Hepatol. 2000; 12:795–798. [PubMed: 10929908]
10. Asaka M, Takeda H, Sugiyama T, Kato M. What role does Helicobacter pylori play in gastric cancer? Gastroenterology. 1997; 113:S56–S60. [PubMed: 9394761]
11. Groopman JD, Kensler TW. Role of metabolism and viruses in aflatoxin-induced liver cancer. Toxicol. Appl. Pharmacol. 2005; 206:131–137. [PubMed: 15967201]
12. Mostafa MH, Sheweita SA, O'Connor PJ. Relationship between schistosomiasis and bladder cancer. Clin. Microbiol. Rev. 1999; 12:97–111. [PubMed: 9880476]
13. Badawi AF, Mostafa MH, Probert A, O'Connor PJ. Role of schistosomiasis in human bladder cancer: evidence of association, aetiological factors, and basic mechanisms of carcinogenesis. Eur. J Cancer Prev. 1995; 4:45–59. [PubMed: 7728097]
14. Visconti R, Grieco D. New insights on oxidative stress in cancer. Curr. Opin. Drug Discov. Devel. 2009; 12:240–245.
15. Dedon PC, Tannenbaum SR. Reactive nitrogen species in the chemical biology of inflammation. Arch. Biochem. Biophys. 2004; 423:12–22. [PubMed: 14989259]
16. Ohshima H, Tatemichi M, Sawa T. Chemical basis of inflammation-induced carcinogenesis. Arch. Biochem. Biophys. 2003; 417:3–11. [PubMed: 12921773]

17. Thomas DD, Ridnour LA, Isenberg JS, Flores-Santana W, Switzer CH, Donzelli S, Hussain P, Vecoli C, Paolocci N, Ambs S, Colton CA, Harris CC, Roberts DD, Wink DA. The chemical biology of nitric oxide: implications in cellular signaling. Free Radic. Biol. Med. 2008; 45:18–31. [PubMed: 18439435]

18. Lancaster J. Nitric oxide in cells. Amer. Sci. 1992; 80:248–259.

19. Hughes MN. Chemistry of nitric oxide and related species. Meth Enz. 2008; 436:3–19.

20. Tretyakova NY, Burney S, Pamir B, Wishnok JS, Dedon PC, Wogan GN, Tannenbaum SR. Peroxynitrite-induced DNA damage in the supF gene: correlation with the mutational spectrum. Mutat. Res. 2000; 447:287–303. [PubMed: 10751613]

21. Bartsch H, Nair J. Oxidative stress and lipid peroxidation-derived DNA-lesions in inflammation driven carcinogenesis. Cancer Detect. Prev. 2004; 28:385–391. [PubMed: 15582261]

22. Blair IA. DNA adducts with lipid peroxidation products. J. Biol. Chem. 2008; 283:15545–15549. [PubMed: 18285329]

23. Mangerich A, Knutson CG, Parry NM, Muthupalani S, Ye W, Prestwich E, Cui L, McFaline JL, Mobley M, Ge Z, Taghizadeh K, Wishnok JS, Wogan GN, Fox JG, Tannenbaum SR, Dedon PC. Infection-induced colitis in mice causes dynamic and tissue-specific changes in stress response and DNA damage leading to colon cancer. Proc. Natl. Acad. Sci. USA. 2012; 109:E1820–E1829. [PubMed: 22689960]

24. Gal A, Tamir S, Kennedy LJ, Tannenbaum SR, Wogan GN. Nitrotyrosine formation, apoptosis, and oxidative damage: relationships to nitric oxide production in SJL mice bearing the RcsX tumor. Cancer Res. 1997; 57:1823–1828. [PubMed: 9157968]

25. Gal A, Tamir S, Tannenbaum SR, Wogan GN. Nitric oxide production in SJL mice bearing the RcsX lymphoma: a model for in vivo toxicological evaluation of NO. Proc. Natl. Acad. Sci. USA. 1996; 93:11499–11503. [PubMed: 8876164]

26. Gal A, Wogan GN. Mutagenesis associated with nitric oxide production in transgenic SJL mice. Proc. Natl. Acad. Sci. USA. 1996; 93:15102–15107. [PubMed: 8986771]

27. Tamir S, deRojas-Walker T, Gal A, Weller AH, Li X, Fox JG, Wogan GN, Tannenbaum SR. Nitric oxide production in relation to spontaneous B-cell lymphoma and myositis in SJL mice. Cancer Res. 1995; 55:4391–4397. [PubMed: 7545539]

28. Slade PG, Slade PG, Williams MV, Chiang A, Iffrig E, Tannenbaum SR, Wishnok JS. A filtered database search algorithm for endogenous serum protein carbonyl modifications in a mouse model of inflammation. Mol. Cell. Proteom. 2011; 10:M111. 007658.

29. Nair J, Gal A, Tamir S, Tannenbaum SR, Wogan GN, Bartsch H. Etheno adducts in spleen DNA of SJL mice stimulated to overproduce nitric oxide. Carcinogenesis. 1998; 19:2081–2084. [PubMed: 9886560]

30. Thorp HH. The importance of being r: greater oxidative stability of RNA compared with DNA. Chem. Biol. 2000; 7:R33–R36. [PubMed: 10662699]

31. Li Z, Wu J, Deleo CJ. RNA damage and surveillance under oxidative stress. IUBMB Life. 2006; 58:581–588. [PubMed: 17050375]

32. Feyzi E, Sundheim O, Westbye MP, Aas PA, Vagbo CB, Otterlei M, Slupphaug G, Krokan HE. RNA base damage and repair. Curr. Pharm. Biotechnol. 2007; 8:326–331. [PubMed: 18289040]

33. Ringvoll J, Moen MN, Nordstrand LM, Meira LB, Pang B, Bekkelund A, Dedon PC, Bjelland S, Samson LD, Falnes PO, Klungland A. AlkB homologue 2-mediated repair of ethenoadenine lesions in mammalian DNA. Cancer Res. 2008; 68:4142–4149. [PubMed: 18519673]

34. Defoiche J, Zhang Y, Lagneaux L, Pettengell R, Hegedus A, Willems L, Macallan DC. Measurement of ribosomal RNA turnover in vivo by use of deuterium-labeled glucose. Clin. Chem. 2009; 55:1824–1833. [PubMed: 19696118]

35. Schmidt EE, Schibler U. Cell size regulation, a mechanism that controls cellular RNA accumulation: consequences on regulation of the ubiquitous transcription factors Oct1 and NF-Y and the liver-enriched transcription factor DBP. J Cell Biol. 1995; 128:467–483. [PubMed: 7532171]

36. Dong M, Wang C, Deen WM, Dedon PC. Absence of 2'-deoxyoxanosine and presence of abasic sites in DNA exposed to nitric oxide at controlled physiological concentrations. Chem. Res. Toxicol. 2003; 16:1044–1055. [PubMed: 12971791]

37. Ryu EK, MacCoss M. New procedure for the chlorination of pyrimidine and purine nucleosides. J. Org. Chem. 1981; 46:2819–2823.
38. Bobalova J, Bobal P, Mutafova-Yambolieva VN. High-performance liquid chromatographic technique for detection of a fluorescent analogue of ADP-ribose in isolated blood vessel preparations. Anal. Biochem. 2002; 305:269–276. [PubMed: 12054456]
39. Chen H. Analysis of 3,N(4)-ethenocytosine in DNA and in human urine by isotope dilution gas chromatography/negative ion chemical ionization mass spectrometry. Chem. Res. Toxicol. 2001; 14:1612–1619. [PubMed: 11743744]
40. Brodie BB, Axelrod J, Shore PA, Udenfriend S. Ascorbic acid in aromatic hydroxylation. II. Products formed by reaction of substrates with ascorbic acid, ferrous ion, and oxygen. J. Biol. Chem. 1954; 208:741–750. [PubMed: 13174583]
41. Singh R, McEwan M, Lamb JH, Santella RM, Farmer PB. An improved liquid chromatography/tandem mass spectrometry method for the determination of 8-oxo-7,8-dihydro-2'-deoxyguanosine in DNA samples using immunoaffinity column purification. Rapid Commun. Mass Spec. 2003; 17:126–134.
42. Taghizadeh K, McFaline JL, Pang B, Sullivan M, Dong M, Plummer E, Dedon PC. Quantification of DNA damage products resulting from deamination, oxidation and reaction with products of lipid peroxidation by liquid chromatography isotope dilution tandem mass spectrometry. Nat. Protoc. 2008; 3:1287–1298. [PubMed: 18714297]
43. E.E.S.C.O.D. Comparative analysis of baseline 8-oxo-7,8-dihydroguanine in mammalian cell DNA, by different methods in different laboratories: An approach to consensus. Carcinogenesis. 2002; 23:2129–2133. [PubMed: 12507938]
44. Dong M, Dedon PC. Relatively small increases in the steady-state levels of nucleobase deamination products in DNA from human TK6 cells exposed to toxic levels of nitric oxide. Chem. Res. Toxicol. 2006; 19:50–57. [PubMed: 16411656]
45. Nishikura K. Functions and regulation of RNA editing by ADAR deaminases. Annu. Rev. Biochem. 2010; 79:321–349. [PubMed: 20192758]
46. Anant S, Blanc V, Davidson NO. Molecular regulation, evolutionary, and functional adaptations associated with C to U editing of mammalian apolipoproteinB mRNA. Progress Nucleic Acid Res. Mol. Biol. 2003; 75:1–41.
47. Gerber AP, Keller W. RNA editing by base deamination: more enzymes, more targets, new mysteries. Trends Biochem. Sci. 2001; 26:376–384. [PubMed: 11406411]
48. Keegan LP, Leroy A, Sproul D, O'Connell MA. Adenosine deaminases acting on RNA (ADARs): RNA-editing enzymes. Genome Biol. 2004; 5:209. [PubMed: 14759252]
49. Su AA, Randau L. A-to-I and C-to-U editing within transfer. RNAs. Biochemistry. 2011; 76:932–937.
50. Chan CT, Dyavaiah M, DeMott MS, Taghizadeh K, Dedon PC, Begley TJ. A quantitative systems approach reveals dynamic control of tRNA modifications during cellular stress. PLoS Genetics. 2010; 6 e1001247.
51. Rio DC, Ares M, Hannon GJ, Nilsen TW. Guidelines for the use of RNA purification kits. Cold Spring Harbor Prot. 2010; 2010 pdb.ip79-pdb.ip79.
52. Chinsky, JM.; Ramamurthy, V.; Knudsen, TB.; Higley, HR.; Fanslow, WC.; Trentin, JJ.; Kellems, RE. Developmental and tissue specific regulation of adenosine deaminase in mice. In: Beudet, AL.; Mulligan, R.; Verma, IM., editors. Gene Transfer and Gene Therapy, Proceedings of an E.I. du Pont de Nemours — UCLA Symposium Held at Tamarron, Colorado, February 6–12, 1988. New York: Alan R. Liss, Inc.; 1989.
53. Chinsky JM, Maa MC, Ramamurthy V, Kellems RE. Adenosine deaminase gene expression. Tissue-dependent regulation of transcriptional elongation. J. Biol. Chem. 1989; 264:14561–14565. [PubMed: 2474547]
54. Paul MS, Bass BL. Inosine exists in mRNA at tissue-specific levels and is most abundant in brain mRNA. EMBO J. 1998; 17:1120–1127. [PubMed: 9463389]
55. Rabinovici R, Kabir K, Chen M, Su Y, Zhang D, Luo X, Yang JH. ADAR1 is involved in the development of microvascular lung injury. Circulation Res. 2001; 88:1066–1071. [PubMed: 11375277]

56. Luo XX, Yang JH, Rabinovici R. Induction of inosine containing mRNA during the inflammatory stress in C57BL/6 mouse. Chinese Sci. Bull. 2003; 48:156–160.
57. Yang JH, Luo X, Nie Y, Su Y, Zhao Q, Kabir K, Zhang D, Rabinovici R. Widespread inosine-containing mRNA in lymphocytes regulated by ADAR1 in response to inflammation. Immunology. 2003; 109:15–23. [PubMed: 12709013]
58. Nevo-Caspi Y, Amariglio N, Rechavi G, Paret G. A-to-I RNA editing is induced upon hypoxia. Shock. 2011; 35:585–589. [PubMed: 21330951]
59. Pang B, McFaline JL, Burgis NE, Dong M, Taghizadeh K, Sullivan MR, Elmquist CE, Cunningham RP, Dedon PC. Defects in purine nucleotide metabolism lead to substantial incorporation of xanthine and hypoxanthine into DNA and RNA. Proc. Natl. Acad. Sci. USA. 2012; 109:2319–2324. [PubMed: 22308425]
60. Benedetti E, Bramanti E, Papineschi F, Rossi I, Benedetti E. Determination of the relative amount of nucleic acids and proteins in leukemic and normal lymphocytes by means of Fourier transform infrared microspectroscopy. Applied Spec. 1997; 51:792–797.
61. Andreeff M, Beck JD, Darzynkiewicz Z, Traganos F, Gupta S, Melamed MR, Good RA. RNA content in human lymphocyte subpopulations. Proc. Natl. Acad. Sci. USA. 1978; 75:1938–1942. [PubMed: 306108]
62. Walle AJ. Distribution and content of nuclear and cellular RNA among cell populations of acute lymphoblastic and nonlymphoblastic leukemia. Cancer Res. 1985; 45:5193–5195. [PubMed: 3861243]
63. Lawrie CH, Gal S, Dunlop HM, Pushkaran B, Liggins AP, Pulford K, Banham AH, Pezzella F, Boultwood J, Wainscoat JS, Hatton CS, Harris AL. Detection of elevated levels of tumour-associated microRNAs in serum of patients with diffuse large B-cell lymphoma. British J. Haemat. 2008; 141:672–675.
64. Kopreski MS, Benko FA, Kwak LW, Gocke CD. Detection of tumor messenger RNA in the serum of patients with malignant melanoma. Clinical Cancer Res. 1999; 5:1961–1965. [PubMed: 10473072]
65. Tong YK, Lo YM. Diagnostic developments involving cell-free (circulating) nucleic acids. Clinica Chim. Acta. 2006; 363:187–196.
66. Laktionov PP, Tamkovich SN, Rykova EY, Bryzgunova OE, Starikov AV, Kuznetsova NP, Sumarokov SV, Kolomiets SA, Sevostianova NV, Vlassov VV. Extracellular circulating nucleic acids in human plasma in health and disease. Nucleosides Nucleotides Nucleic Acids. 2004; 23:879–883. [PubMed: 15560076]
67. Rykova, EY.; Laktionov, PP.; Vlassov, VV. Circulating Nucleic Acids in Health and Disease. In: Kikuchi, Y.; Rykova, EY., editors. Extracellular Nucleic Acids. Berlin Heidelberg: Springer-Verlag; 2010. p. 93-128.
68. Morozkin ES, Laktionov PP, Rykova EY, Bryzgunova OE, Vlassov VV. Release of nucleic acids by eukaryotic cells in tissue culture. Nucleosides Nucleotides Nucleic Acids. 2004; 23:927–930. [PubMed: 15560083]
69. Gahan, PB.; Stroun, M. The biology of circulating nucleic acids in plasma and serum (CNAPS). In: Kikuchi, Y.; Rykova, EY., editors. Extracellular Nucleic Acids. Berlin Heidelberg: Springer-Verlag; 2010. p. 167-189.
70. Kuligina EV, Vratskih OV, Semenov DV, Matveeva VA, Richter VA. Deamination of adenosines in extracellular RNA spontaneously internalized by human cells. Annals New York Acad. Sci. 2008; 1137:51–57.
71. Kong Q, Shan X, Chang Y, Tashiro H, Lin CL. RNA oxidation: a contributing factor or an epiphenomenon in the process of neurodegeneration. Free Rad. Res. 2008; 42:773–777.
72. Saxowsky TT, Meadows KL, Klungland A, Doetsch PW. 8-Oxoguanine-mediated transcriptional mutagenesis causes Ras activation in mammalian cells. Proc. Natl. Acad. Sci. U S A. 2008; 105:18877–18882. [PubMed: 19020090]
73. Wang Q, Zhang Z, Blackwell K, Carmichael GG. Vigilins bind to promiscuously A-to-I-edited RNAs and are involved in the formation of heterochromatin. Current Biol. 2005; 15:384–391.

74. Chan CTY, Pang YLJ, Deng W, Babu IR, Dyavaiah M, Begley TJ, Dedon PC. Reprogramming of tRNA modifications controls the oxidative stress response by codon-biased translation of proteins. Nature Commun. 2012; 3:937. [PubMed: 22760636]
75. Anderson P. Post-transcriptional control of cytokine production. Nature Immunol. 2008; 9:353–359. [PubMed: 18349815]
76. Kleinert H, Schwarz PM, Forstermann U. Regulation of the expression of inducible nitric oxide synthase. Biol. Chem. 2003; 384:1343–1364. [PubMed: 14669979]
77. Kleinert H, Pautz A, Linker K, Schwarz PM. Regulation of the expression of inducible nitric oxide synthase. European J. Pharmacol. 2004; 500:255–266. [PubMed: 15464038]
78. Paz-Yaacov N, Levanon EY, Nevo E, Kinar Y, Harmelin A, Jacob-Hirsch J, Amariglio N, Eisenberg E, Rechavi G. Adenosine-to-inosine RNA editing shapes transcriptome diversity in primates. Proc. Natl. Acad. Sci. USA. 2010; 107:12174–12179. [PubMed: 20566853]
79. Linker K, Pautz A, Fechir M, Hubrich T, Greeve J, Kleinert H. Involvement of KSRP in the post-transcriptional regulation of human iNOS expression-complex interplay of KSRP with TTP and HuR. Nucleic Acids Res. 2005; 33:4813–4827. [PubMed: 16126846]
80. Lisi L, Navarra P, Feinstein DL, Dello Russo C. The mTOR kinase inhibitor rapamycin decreases iNOS mRNA stability in astrocytes. J. Neuroinflam. 2011; 8:1.
81. von Roretz C, Di Marco S, Mazroui R, Gallouzi IE. Turnover of AU-rich-containing mRNAs during stress: a matter of survival. Wiley Interdisc. Rev. RNA. 2011; 2:336–347.
82. Ma CH, Chong JH, Guo Y, Zeng HM, Liu SY, Xu LL, Wei J, Lin YM, Zhu XF, Zheng GG. Abnormal expression of ADAR1 isoforms in Chinese pediatric acute leukemias. Biochem. Biophys. Res. Commun. 2011; 406:245–251. [PubMed: 21316340]
83. Steinman RA, Yang Q, Gasparetto M, Robinson LJ, Liu X, Lenzner DE, Hou J, Smith C, Wang Q. Deletion of the RNA-editing enzyme ADAR1 causes regression of established chronic myelogenous leukemia in mice. Int. J. Cancer. 2013; 132:1741–1750. [PubMed: 22987615]
84. Hofer T, Badouard C, Bajak E, Ravanat JL, Mattsson A, Cotgreave IA. Hydrogen peroxide causes greater oxidation in cellular RNA than in DNA. Biol. Chem. 2005; 386:333–337. [PubMed: 15899695]
85. Hofer T, Seo AY, Prudencio M, Leeuwenburgh C. A method to determine RNA and DNA oxidation simultaneously by HPLC-ECD: Greater RNA than DNA oxidation in rat liver after doxorubicin administration. Biol. Chem. 2006; 387:103–111. [PubMed: 16497170]
86. Shen Z, Wu W, Hazen SL. Activated leukocytes oxidatively damage DNA, RNA, and the nucleotide pool through halide-dependent formation of hydroxyl radical. Biochemistry. 2000; 39:5474–5482. [PubMed: 10820020]
87. Weyand EH, Bevan DR. Covalent binding of benzo[a]pyrene to macromolecules in lung and liver of rats following intratracheal instillation. Cancer Lett. 1987; 36:149–159. [PubMed: 2441851]
88. Miller JA, Miller EC. The metabolic activation and nucleic acid adducts of naturally-occurring carcinogens: recent results with ethyl carbamate and the spice flavors safrole and estragole. Br. J. Cancer. 1983; 48:1–15. [PubMed: 6191767]
89. Sotomayor RE, Washington M, Nguyen L, Nyang'anyi R, Hinton DM, Chou M. Effects of intermittent exposure to aflatoxin B1 on DNA and RNA adduct formation in rat liver: dose-response and temporal patterns. Toxicol. Sci. 2003; 73:329–338. [PubMed: 12700393]
90. Wang M, Hecht SS. A cyclic N7,C-8 guanine adduct of N-nitrosopyrrolidine (NPYR): formation in nucleic acids and excretion in the urine of NPYR-treated rats. Chem. Res. Toxicol. 1997; 10:772–778. [PubMed: 9250411]
91. Fernando RC, Nair J, Barbin A, Miller JA, Bartsch H. Detection of 1,N^6-ethenodeoxyguanosine and 3,N^4-ethenodeoxycytidine by immunoaffinity/^{32}P-post-labelling in liver and lung DNA of mice treated with ethyl carbamate (urethane) or its metabolites. Carcinogenesis. 1996; 17:1711–1718. [PubMed: 8761431]
92. Fiala ES, Conaway CC, Mathis JE. Oxidative DNA and RNA damage in the livers of Sprague-Dawley rats treated with the hepatocarcinogen 2-nitropropane. Cancer Res. 1989; 49:5518–5522. [PubMed: 2477143]
93. Zhu P, Lee SH, Wehrli S, Blair IA. Characterization of a lipid hydroperoxide-derived RNA adduct in rat intestinal epithelial cells. Chem. Res. Toxicol. 2006; 19:809–817. [PubMed: 16780360]

94. Badouard C, Masuda M, Nishino H, Cadet J, Favier A, Ravanat JL. Detection of chlorinated DNA and RNA nucleosides by HPLC coupled to tandem mass spectrometry as potential biomarkers of inflammation. J. Chromatogr. B Analyt. Technol. Biomed. Life Sci. 2005; 827:26–31.

95. Gan W, Nie B, Shi F, Xu XM, Qian JC, Takagi Y, Hayakawa H, Sekiguchi M, Cai JP. Age-dependent increases in the oxidative damage of DNA, RNA, and their metabolites in normal and senescence-accelerated mice analyzed by LC-MS/MS: urinary 8-oxoguanosine as a novel biomarker of aging. Free Radic. Biol. Med. 2012; 52:1700–1707. [PubMed: 22348977]

96. Arczewska KD, Kusmierek JT. Bacterial DNA repair genes and their eukaryotic homologues: 2. Role of bacterial mutator gene homologues in human disease. Overview of nucleotide pool sanitization and mismatch repair systems. Acta Biochim. Pol. 2007; 54:435–457. [PubMed: 17893750]

97. Burgis NE, Cunningham RP. Substrate specificity of RdgB protein, a deoxyribonucleoside triphosphate pyrophosphohydrolase. J. Biol. Chem. 2007; 282:3531–3538. [PubMed: 17090528]

98. Tsuchimoto D, Iyama T, Nonaka M, Abolhassani N, Ohta E, Sakumi K, Nakabeppu Y. A comprehensive screening system for damaged nucleotide-binding proteins. Mutat. Res. 2010; 703:37–42. [PubMed: 20542141]

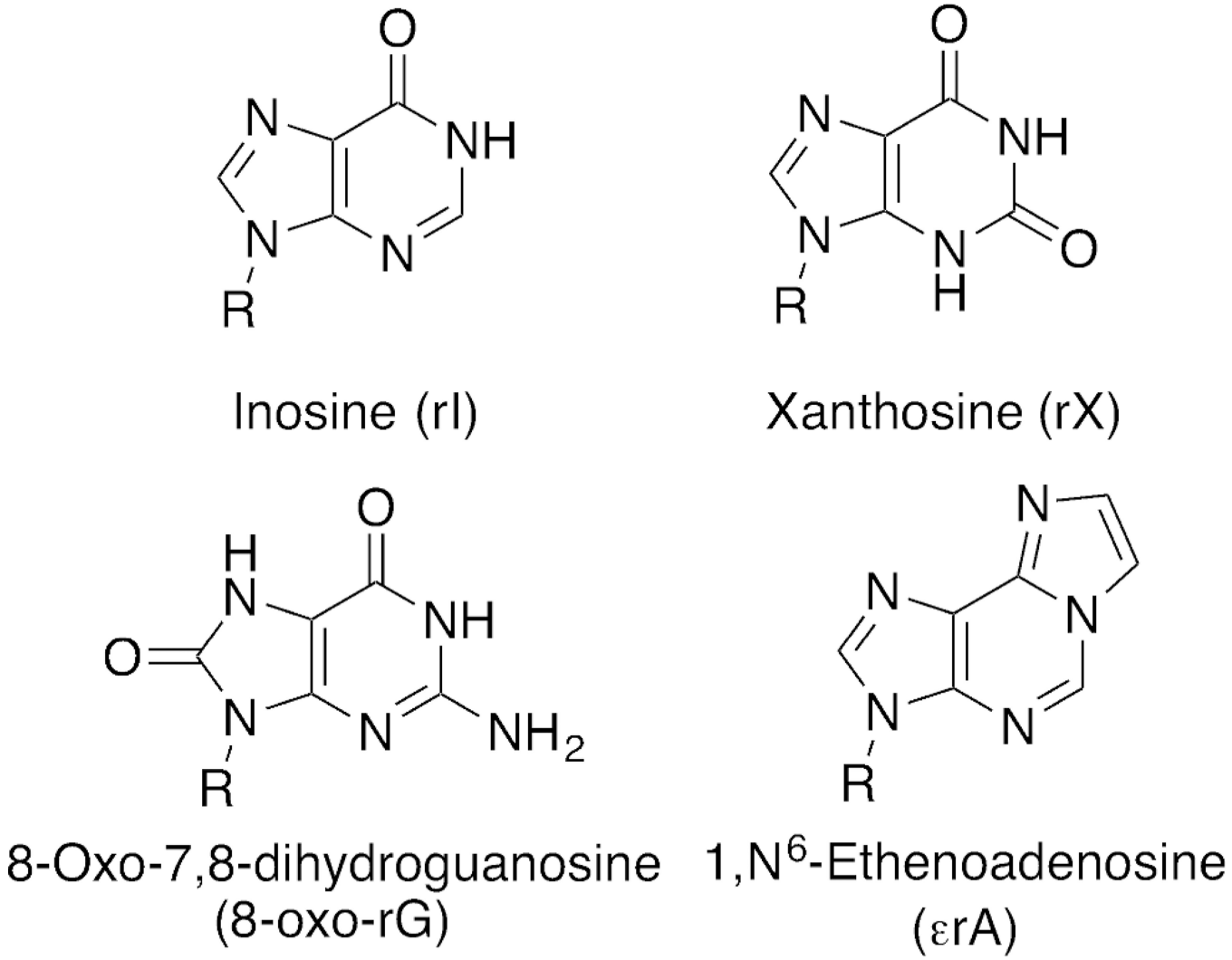

Figure 1.
Inflammation-induced nucleobase damage products.

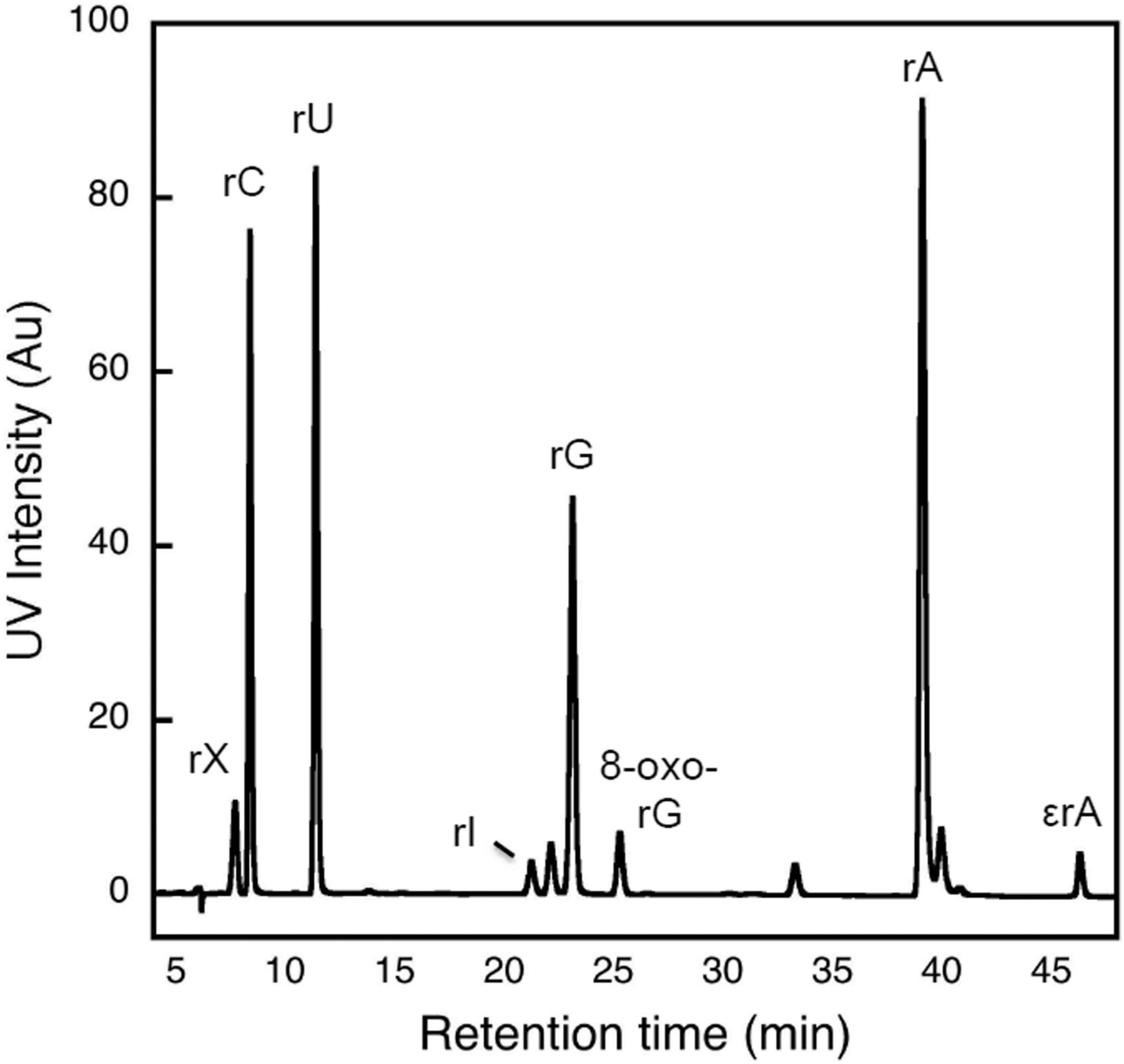

Figure 2.
HPLC chromatogram demonstrating the separation of ribonucleoside forms of RNA damage products.

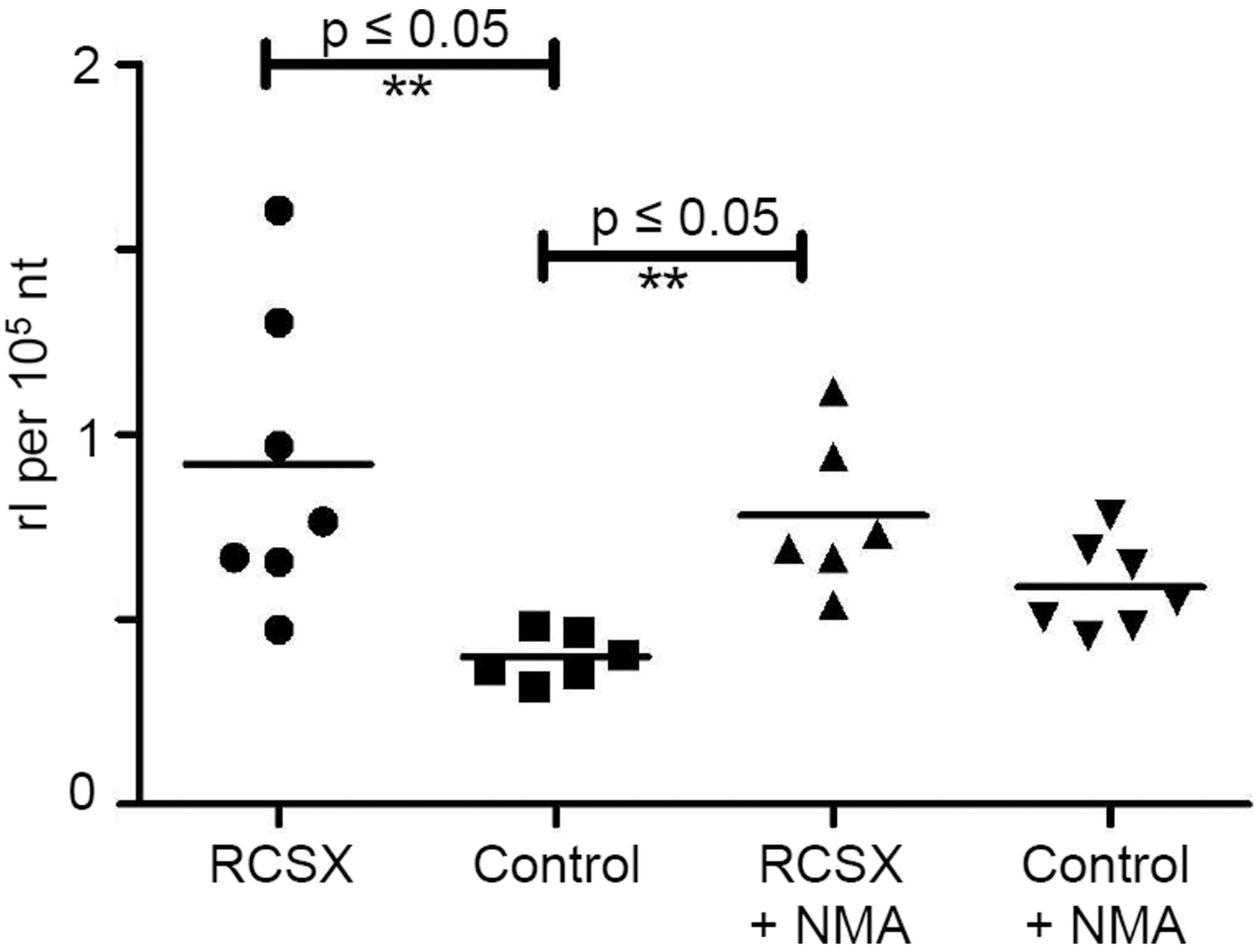

Figure 3.
Comparisons of rI levels in spleen. Asterisks indicate statistically significant differences by the Mann-Whitney t-test ($p < 0.05$).

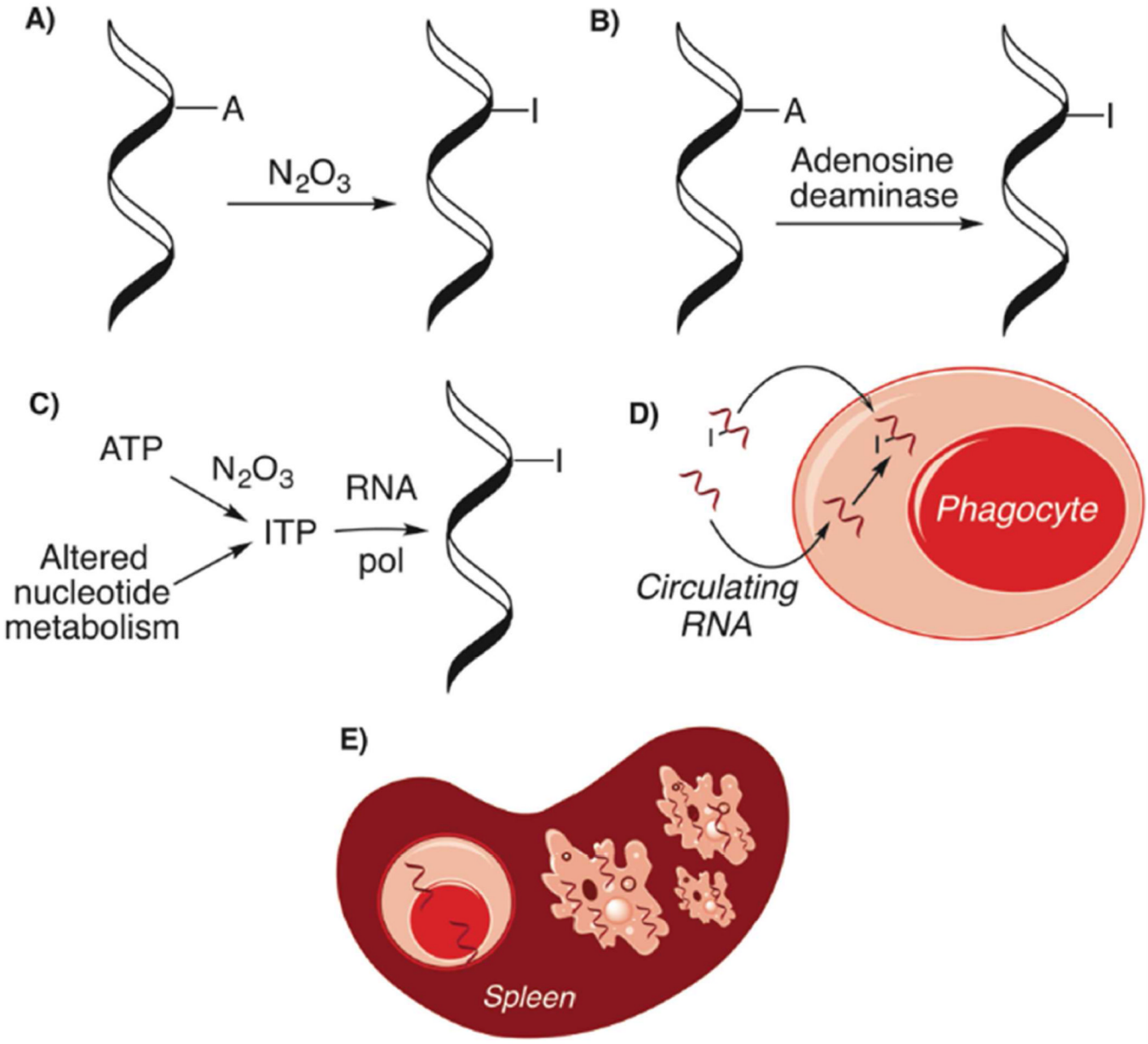

Figure 4. Potential Mechanisms for increased rI in inflamed SJL mouse spleen. (A) Chemical deamination by nitrous anhydride (N_2O_3) reaction with RNA. (B) Enzymatic deamination by adenosine deaminase or other deaminases. (C) Chemical deamination by nitrous anhydride (N_2O_3) reaction with components of the nucleotide pool or altered nucleotide metabolism. (D) Uptake of circulating tumor cell RNA by phagocytes that accumulate in the spleen. (E) Changes in cellular composition of the spleen as a result of RcsX cell treatment in the SJL mouse

Table 1

Levels of RNA damage products in spleen, liver, and kidney tissue[a]

Organ	Treatment	Nitrosation		Lipid Peroxidation	Oxidation
		rX per 10^7 (n)	rI per 10^6 (n)	εrA per 10^8 (n)	8-oxo-rG per 10^5 (n)
Spleen	Control	2.0 ± 0.3 (9)	4.0 ± 0.6 (6)	2.4 ± 0.4 (9)	1.2 ± 0.5 (9)
	Control + NMA	1.9 ± 0.3 (9)	5.9 ± 1.1 (7)	2.4 ± 0.2 (9)	1.5 ± 0.8 (8)
	RcsX	1.8 ± 0.1 (8)	9.2 ± 3.7[b] (7)	2.5 ± 0.4 (9)	1.5 ± 1.0 (9)
	RcsX + NMA	1.8 ± 0.1 (8)	7.8 ± 1.9 (6)	2.2 ± 0.15 (8)	1.3 ± 0.3 (9)
Liver	Control	2.8 ± 0.1 (9)	1.9 ± 0.6 (9)	4.7 ± 1.9 (7)	1.4 ± 0.4 (8)
	Control + NMA	1.8 ± 0.2 (8)	2.1 ± 0.7 (9)	4.7 ± 1.7 (8)	1.5 ± 0.4 (9)
	RcsX	2.0 ± 0.5 (8)	2.0 ± 0.9 (8)	3.8 ± 0.5 (7)	1.1 ± 0.2 (9)
	RcsX + NMA	3.8 ± 1.8 (9)	5.5 ± 5.7 (9)	4.3 ± 3.4 (6)	1.2 ± 0.3 (9)
Kidney	Control	2.0 ± 0.2 (9)	6.5 ± 0.5 (6)	4.1 ± 0.9 (9)	1.7 ± 1.4 (9)
	Control + NMA	2.0 ± 0.2 (8)	5.7 ± 1.6 (5)	3.5 ± 0.9 (9)	1.3 ± 1.2 (9)
	RcsX	2.0 ± 0.1 (8)	7.2 ± 0.8 (5)	4.3 ± 1.5 (8)	0.9 ± 1.2 (9)
	RcsX + NMA	2.4 ± 2.0 (9)	7.3 ± 0.5 (6)	3.4 ± 0.6 (9)	0.6 ± 1.0 (9)

[a] Values represent the mean ± SD, N as marked. Outliers were determined and removed using the Grubbs test.

[b] RcsX-treated sample significantly different from control by Student's and Mann-Whitney t-tests ($p < 0.05$).

Table 2

Ratio of RNA damage to DNA damage in SJL mouse tissues[a]

Tissue	Etheno-A per 10^8 nt		8-oxo-G per 10^6 nt		Xanthine per 10^7 nt		Hypoxanthine per 10^6 nt	
	Control	RcsX	Control	RcsX	Control	RcsX	Control	RcsX
Spleen	2.1	0.56	10	12	0.34	0.23	2.9	5.8
Liver	2.4	1.2	11	9.2	0.58	0.34	1.6	1.4
Kidney	2.7	1.0	-	-	0.38	0.40	5.4	6.5

[a]RNA data from Table 1, DNA data from Pang *et al.*[1] Values represent ratio of RNA to DNA.